

Dihydroceramide-based Response to Hypoxia*

Received for publication, August 25, 2011, and in revised form, September 12, 2011. Published, JBC Papers in Press, September 13, 2011, DOI 10.1074/jbc.M111.297994

Cecilia M. Devlin[‡], Tim Lahm^{‡§}, Walter C. Hubbard[¶], Mary Van Demark[‡], Kevin C. Wang[‡], Xue Wu^{||}, Alicja Bielawska^{**}, Lina M. Obeid^{**}, Mircea Ivan^{¶||1}, and Irina Petrace^{‡§2}

From the Departments of [‡]Medicine and ^{||}Microbiology and Immunology, Indiana University, Indianapolis, Indiana 46202, [§]R. L. Roudebush Veterans Affairs Medical Center, Indianapolis, Indiana 46202, [¶]Department of Medicine, The Johns Hopkins University, Baltimore, Maryland 21286, and ^{**}Department of Pediatrics, Medical University of South Carolina, Charleston, South Carolina 29425

Background: The role of the oxygen-dependent dihydroceramide desaturases during hypoxia is unknown.

Results: Desaturases are rapidly, directly, and reversibly inhibited by hypoxia, independently of hypoxia-inducible factor, markedly increasing dihydroceramides that in turn inhibit cell proliferation.

Conclusion: Desaturase activity alters the balance of dihydroceramides/ceramides, regulating cell proliferation in hypoxia/reoxygenation.

Significance: Dihydroceramide desaturases are oxygen biosensors generating dihydroceramides that may be useful as hypoxia biomarkers.

To understand the mechanisms of ceramide-based responses to hypoxia, we performed a mass spectrometry-based survey of ceramide species elicited by a wide range of hypoxic conditions (0.2–5% oxygen). We describe a rapid, time-dependent, marked up-regulation of dihydroceramides (DHCs) in mammalian cells and in the lungs of hypoxic rats. The increase affected all DHC species and was proportional with the depth and duration of hypoxia, ranging from 2- (1 h) to 10-fold (24 h), with complete return to normal after 1 h of reoxygenation at the expense of increased ceramides. We demonstrate that a DHC-based response to hypoxia occurs in a hypoxia-inducible factor-independent fashion and is catalyzed by the DHC desaturase (DEGS) in the *de novo* ceramide pathway. Both the impact of hypoxia on DHC molecular species and its inhibitory effect on cell proliferation were reproduced by knockdown of DEGS1 or DEGS2 by siRNA during normoxia. Conversely, overexpression of DEGS1 or DEGS2 attenuated the DHC accumulation and increased cell proliferation during hypoxia. Based on the amplitude and kinetics of DHC accumulation, the enzymatic desaturation of DHCs fulfills the criteria of an oxygen sensor across physiological hypoxic conditions, regulating the balance between biologically active components of ceramide metabolism.

Hypoxia elicits diverse and insufficiently understood effects on lipid metabolism, including modulation of lipid second messengers, such as ceramides (1). The molecular basis for oxygen sensing in the ceramide biosynthesis pathway *in vivo* is not well characterized. The complex cellular adaptation to hypoxia includes responses controlled by hypoxia-inducible factors

(HIFs),³ which are directly regulated by the prolyl and asparaginyl hydroxylase oxygen sensors (2). However, an increasing variety of HIF-independent responses to hypoxia have been described (3). We set out to determine the mechanisms by which hypoxia impacts the synthesis of ceramides across a physiological range of oxygen concentrations *in vivo*.

Several important biological consequences have been attributed to ceramide species, including regulation of cell growth, differentiation, and apoptosis (3). Ceramides have recently received attention in the context of hypoxia response in the model organism *Caenorhabditis elegans* (4). This study provided an important first step toward understanding the role of sphingolipids in the hypoxia responses of mammalian cells. Previous reports indicated that ceramides are increased in specific organs of animals exposed to chronic hypoxia; however, these changes may be indirectly associated with oxygen deprivation (5). Some studies using cultured rat cortical neurons have shown that the level of ceramides increases upon reoxygenation after hypoxia (6, 7). Additionally, earlier studies typically relied on assays that are less than ideal for distinguishing between the various ceramide species, and therefore, rather limited mechanistic insight has been generated. Ceramide synthesis is regulated at the level of sphingomyelin hydrolysis via sphingomyelinases or through the *de novo* pathway via serine palmitoyltransferase and (dihydro)ceramide synthases, which produce dihydroceramide (DHC), a substrate for desaturases to generate ceramide. Ceramide levels can also be modulated by ceramidase-mediated catabolism to sphingosine or the recycling of sphingosine back to ceramides (8). Both *de novo* ceramide synthesis (9) and sphingomyelinase-mediated ceramide production (10) have been reported in the activation of ceramide responses to hypoxia in addition to an inhibition of the intracellular ceramide transport during oxygen deprivation

* This work was supported, in whole or in part, by National Institutes of Health Grants RO1HL077328 (to I. P.) and 1 S10 RR16798 (to W. C. H. for funding the API4000 LC-MS/MS system).

¹ To whom correspondence may be addressed: Indiana University, 980 W. Walnut St., Walther Hall C225, Indianapolis, IN 46202. Tel.: 317-274-0322; E-mail: mivan@iupui.edu.

² To whom correspondence may be addressed: Indiana University, 980 W. Walnut Street, Walther Hall C400, Indianapolis, IN 46202. Tel.: 317-278-2894; Fax: 317-988-3976; E-mail: ipetrach@iupui.edu.

³ The abbreviations used are: HIF, hypoxia-inducible factor; DHC, dihydroceramide; DEGS, DHC desaturase; C₁₂-dhCCPS, D-erythro-2-N-[12'-(1"-pyridinium)dodecanoyl]-4,5-dihydro-sphingosine bromide; C₁₂-CCPS, D-erythro-2-N-[12'-(1"-pyridinium)dodecanoyl]sphingosine bromide; Vec, vector; VHL, von Hippel-Lindau.

Mechanism of Hypoxia-induced DHC

(11), depending on the cell type and the injury type (ischemia versus hypoxia). Despite the knowledge that the desaturases are oxygen-dependent enzymes, there is little known about their response across physiological ranges of oxygen concentration in live cells or tissues or if they are impacted by other metabolic consequences of hypoxia, such as shifts in the NADH/NAD balance that occur *in vivo*. Furthermore, the biological significance of the sphingolipids generated during hypoxia remains under debate (12) with certain ceramide species being implicated in apoptosis and others being implicated in cell survival. The portrayal of DHCs as biologically inactive ceramide precursors has recently been challenged (13–15); furthermore, their role in hypoxic responses remains unknown.

To gain a deeper understanding of ceramide-based responses to decreased oxygen tension, we performed a mass spectrometry-based, comprehensive survey of the ceramide species produced under hypoxic conditions in multiple mammalian cell types and *in vivo*. We report that cellular sensing of hypoxia involves a rapid up-regulation of DHC in a non-transcriptional, dose-dependent but HIF-independent manner that may in turn regulate the cell proliferation response to low oxygen tension.

EXPERIMENTAL PROCEDURES

Reagents—All chemical reagents were purchased from Sigma-Aldrich unless otherwise stated. Ceramides (C12:0) and dihydroceramide (DHC 8:0) were purchased from Avanti Polar Lipids (Alabaster, AL). Dimethylxalylglycine was purchased from Frontier Scientific (Logan, UT) and prepared in dimethyl sulfoxide.

DHC Analog—The dihydroceramidoid D-erythro-2-N-[12'-(1"-pyridinium)dodecanoyl]-4,5-dihydrosphingosine bromide (C₁₂-dhCCPS; LCL249) and the corresponding ceramidoid (C₁₂-CCPS; LCL88) were prepared as described previously (15).

Plasmids—pCMV6, a FLAG-tagged empty vector (RC123456, OriGene Technologies Inc., Rockville, MD); DEGS2.pCMV (RC217308, OriGene Technologies, Inc.), a pCMV6 vector containing cDNA for human *DEGS2*; EGFP.M14 (EX-EGFP-M14, GeneCopoeia, Rockville, MD), a pReceiver-M14 plasmid containing enhanced GFP cDNA and a FLAG tag; and DEGS1.M14 (EX-I0056-M14, GeneCopoeia), a pReceiver-M14 plasmid containing *DEGS1* cDNA were used.

Cell Lines—MCF-7, MDA231, and 468 human breast cancer cell lines grown in DMEM were from ATCC (Manassas, VA). A549 human lung cancer cells were from Dr. John Turchi (Indiana University). Transformed human lung bronchial epithelial cells (Beas2B) were from Dr. Augustine M. K. Choi (Harvard University). Primary rat lung microvascular endothelial cells were from Dr. Troy Stevens (University of Southern Alabama). Wild-type or HIF_{1 α} -deficient murine embryonic fibroblasts (16) were from Dr. Meredith Crosby (Yale University). Renal clear cell carcinoma cells 786-O Vec and 786-O WT (17) grown in DMEM/Ham's F-12 (1:1) and G418 (200 μ g/ml) were from Dr. Maria Czyzyk-Krzeska (University of Cincinnati). Cells were maintained in their respective medium containing 10% fetal bovine serum and cultured at 37 °C in 5% CO₂ and 95% air.

Exposure to Hypoxia of Cultured Cells—Cells were plated in 35-mm plastic dishes for 24 h and then incubated in either normoxic (21% O₂) or hypoxic (0.2, 1, or 5% O₂) conditions for

the indicated time. Hypoxic conditions were maintained in an InVivo200 (Ruskin, Inc., Cincinnati, OH) hypoxia work station. Following exposure, cells were washed with cold PBS and processed for end point analyses. Reoxygenation effects were tested by exposure to hypoxic conditions (0.2% O₂ for 24 h) followed by transfer of cell culture plates to normoxic conditions.

Cell Proliferation—Cell proliferation was tested by measuring BrdU incorporation into DNA using Cell Proliferation ELISA BrdU colorimetric assays (Roche Diagnostics).

siRNA Knockdown Experiments—For HIF knockdown, MCF-7 cells were reverse transfected with either HIF_{1 α} -, HIF_{2 α} - (5 nM), or negative control siRNA (Ambion, Inc., Austin, TX) using siPORT NeoFX transfection reagent according to the manufacturer's instructions. For DEGS1 or DEGS2 knockdown, MCF-7 or A549 cells were transfected with either DEGS1, DEGS2 (10 or 20 nM), or negative control siRNA (Ambion, Inc.) using Lipofectamine 2000 (Invitrogen) according to the manufacturer's instructions. Twenty-four hours following transfections, the medium was changed, and cells were subjected to experimental conditions.

Animal Studies—The Animal Care and Use Committee of the Indiana University School of Medicine approved all experimental procedures. Male Sprague-Dawley rats were obtained from Charles River Laboratories (Wilmington, MA). All animals were allowed food and water *ad libitum* for at least 7 days in a non-stressful environment prior to experimentation. Animals underwent a 12-h light-dark cycle. Rats (9–16 weeks old; 300–400 g) were exposed to hypoxia (fraction of inspired O₂, 5%) using a dilution chamber. At the end of the hypoxia exposure or after reoxygenation, respectively, animals were sacrificed using isoflurane overdose. In animals that underwent hypoxia without reoxygenation, this was performed while the rats remained in a hypoxic environment. Lungs were harvested immediately and snap frozen in liquid nitrogen for further ceramide and DHC determination.

Ceramide and DHC Determination—Lipid extraction and total lipid phosphorus (P_i) measurements were carried out using a modified Bligh and Dyer method (18) and lipid P_i determination (19), respectively, as described previously (20). Sphingolipid analyses were performed via combined liquid chromatography-tandem mass spectrometry (LC-MS/MS) using an API4000 Q-trap hybrid triple quadrupole linear ion trap mass spectrometer (Applied Biosystems/MDS SCIEX) equipped with turbo ion spray ionization source and Agilent 1100 series liquid chromatography as a front end (Agilent Technologies, Wilmington, DE). The following individual molecular species of ceramide were monitored: 14:0, 16:0, 18:0, 18:1, 20:0, 24:0, and 24:1 ceramide; C₁₇-ceramide was used as an internal standard. Ceramide measurements were normalized by total lipid phosphorus.

DHC Desaturase Activity Assay—MCF-7 cells were exposed to hypoxia in the presence of 10 μ M C₁₂-dhCCPS, and the activity of DHC desaturase was quantified by monitoring the rate of conversion of C₁₂-dhCCPS to C₁₂-CCPS as described previously (15) using an API4000 Q-trap hybrid triple quadrupole linear ion trap mass spectrometer.

Quantitative PCR Analysis of mRNA Levels—RNA was extracted from cells using an miRNeasy kit (Qiagen, Valencia, CA). First strand cDNA was obtained from RNA using random hexamers and MultiScribe reverse transcriptase (Applied Biosystems, Foster City, CA). Quantitative PCR was performed using TaqMan Gene Expression assays and Universal PCR Master Mix (Applied Biosystems) in a 7900HT Sequence Detection System (Applied Biosystems). The relative quantitative mRNA level was determined using the comparative C_t method using 18 S rRNA as the reference gene (21).

Ceramide Synthesis Inhibition Studies—Myriocin, the pharmacological inhibitor of serine palmitoyltransferase (50 nM for 2 h; Biomol International, Plymouth Meeting, PA) was used.

Overexpression of Desaturase (DEGS) in MCF-7 Cells—To overexpress either *DEGS1* or *DEGS2* in MCF-7 cells, the cells were transfected with plasmids containing the appropriate cDNA or the control plasmid. For transient transfection, MCF-7 cells in 35-mm wells were transfected with 10 μ g of plasmid DNA (pCMV6, *DEGS2*.pCMV, EGFP.M14, or *DEGS1*.M14). For stable transfection, MCF-7 cells were transfected with the above plasmids and selected for growth in G418 (0.5 mg/ml).

Western Blot Analysis of Overexpressed DEGS Proteins—Equal amounts of protein were separated by electrophoresis in 10–20% Tris-glycine gels (Invitrogen) and transferred to 0.45- μ m nitrocellulose membranes (Thermo Scientific), which were incubated with a rabbit polyclonal antibody to FLAG tag (1:4000 dilution; Abcam, Cambridge, MA). The chemiluminescence signal was detected following incubation with HRP-linked secondary antibody (Abcam).

Statistical Analysis—Statistical analysis was performed using SigmaStat 3.5. Comparisons among groups were made using analysis of variance. For experiments in which two conditions were being compared, a two-tailed Student's *t* test was used. Statistically significant differences were considered if *p* values were <0.05.

RESULTS

Dose- and Time-dependent Up-regulation of DHC in Response to Hypoxia in Vitro and in Vivo—Exposure to hypoxia for up to 48 h triggered a highly reproducible and robust increase of DHC in all cell types tested, such as breast carcinoma cell lines MCF-7 (Fig. 1A), 468, and MDA231 (data not shown); mouse embryonic fibroblasts (not shown); transformed lung bronchial epithelial cell line Beas2B (Fig. 1B); and primary rat lung microvascular endothelial cells (Fig. 1C). The elevation of total cellular DHC occurred in a time- and dose-dependent fashion (Fig. 1, D and E); it was significantly up-regulated by mild hypoxia (5% O₂) as early as 4 h and reached a 5-fold increase after 24 h of profound hypoxia exposure (0.2% O₂). In contrast, total ceramide levels either did not change or were even slightly decreased in response to a similar oxygen concentration (Fig. 1E). Of the DHC species measured, the earliest changes in response to hypoxia were noted in DHC 24:1 and 24:0, which exhibited a significant up-regulation (2-fold) as early as 1 h following exposure to hypoxia (0.2% O₂; data not shown). The absolute levels of all DHC species were found to be up-regulated, leading to marked increases in the DHC/cer-

amide ratios in cells exposed to low oxygen tension (0.2% for 24 h; Fig. 1F). To ensure that biologically relevant levels of hypoxia were attained in these cells, we utilized two biomarkers, miR-210 (not shown) and carbonic anhydrase 9 mRNA, which exhibited a marked up-regulation after exposure to 4 h of profound hypoxia (0.2% O₂) or 24 h of mild hypoxia (5% O₂), respectively (Fig. 1G).

DHC levels promptly and significantly decreased following removal from hypoxia as early as 1 h, returning to normoxic levels by 4 h of reoxygenation (21% O₂; Fig. 2A). Interestingly, the relative abundance of ceramides *versus* DHC changed dramatically and differentially during hypoxia as compared with reoxygenation. Whereas hypoxia exposure reduced the typical ceramide/DHC ratio of 12:1 found in normoxic cells to 1.2:1 (Fig. 2B), the subsequent exposure to normal oxygen tension significantly increased ceramide/DHC ratios to 8:1 in a time-dependent manner (Fig. 2B). Importantly, a similar sphingolipid response to hypoxia was observed *in vivo* in a rat model of acute hypoxia. Adult rats were exposed to either normoxia or hypoxia (5% O₂) for 60 min. Lungs were harvested immediately following hypoxia exposure or following 60 min of reoxygenation. Hypoxia exposure reduced the ceramide/DHC ratio compared with normoxia, whereas reoxygenation not only restored this fraction but led to a higher ceramide/DHC ratio than that in normoxia (Fig. 2C). Together, these results suggested a hypoxia-sensitive molecular switch that turns off the DHC metabolism to ceramide in hypoxia followed by its restoration upon reoxygenation.

Mechanisms of DHC and Ceramide Balance Alteration in Hypoxia—DHCs are generated via *de novo* biosynthesis and then converted to ceramides by the incorporation of a 4,5-*trans* double bond by DHC desaturase (DEGS) (22, 23), a process mainly located within the endoplasmic reticulum. To investigate whether DEGS activity is modulated by hypoxia *in vivo*, we utilized a recently established mass spectrometry-based method using cell-permeable DHC analogs (dhCCPS) (14). C₁₂-dhCCPS is a substrate for the endogenous DEGS; thus, its conversion to C₁₂-CCPS can be quantitatively tracked. Exposure to hypoxia (0.2% O₂ for 24 h) profoundly and significantly blocked cellular DEGS activity (Fig. 3A). The effect on the desaturase was time- and O₂ concentration-dependent (Fig. 3, B and C); its activity was decreased by almost 50% after 1 h of profound hypoxia (0.2% O₂; Fig. 3B) or after 24 h of mild hypoxia (5% O₂; Fig. 3C) and was abolished after 24 h of severe hypoxia (1% O₂; Fig. 3C). Interestingly, the regulation of DEGS by hypoxia did not occur at a transcriptional level because the levels of both *DEGS1* and *DEGS2* mRNA in hypoxia actually increased following prolonged exposure to low oxygen tension (Fig. 3D).

The mechanistic role of the *de novo* ceramide pathway in the hypoxia-induced DHC increase was interrogated using myriocin, a specific serine palmitoyltransferase inhibitor. Myriocin (Fig. 3E) attenuated hypoxia-induced DHC up-regulation. Furthermore, effective inhibition of *DEGS1* or *DEGS2* using specific siRNAs (Fig. 3, F–H) during normoxia reproduced the effects of low oxygen tension by significantly increasing DHC (Fig. 3I) and markedly increasing DHC/ceramide ratios (Fig. 3J). During hypoxia exposure, inhibition of *DEGS1* caused an

Mechanism of Hypoxia-induced DHC

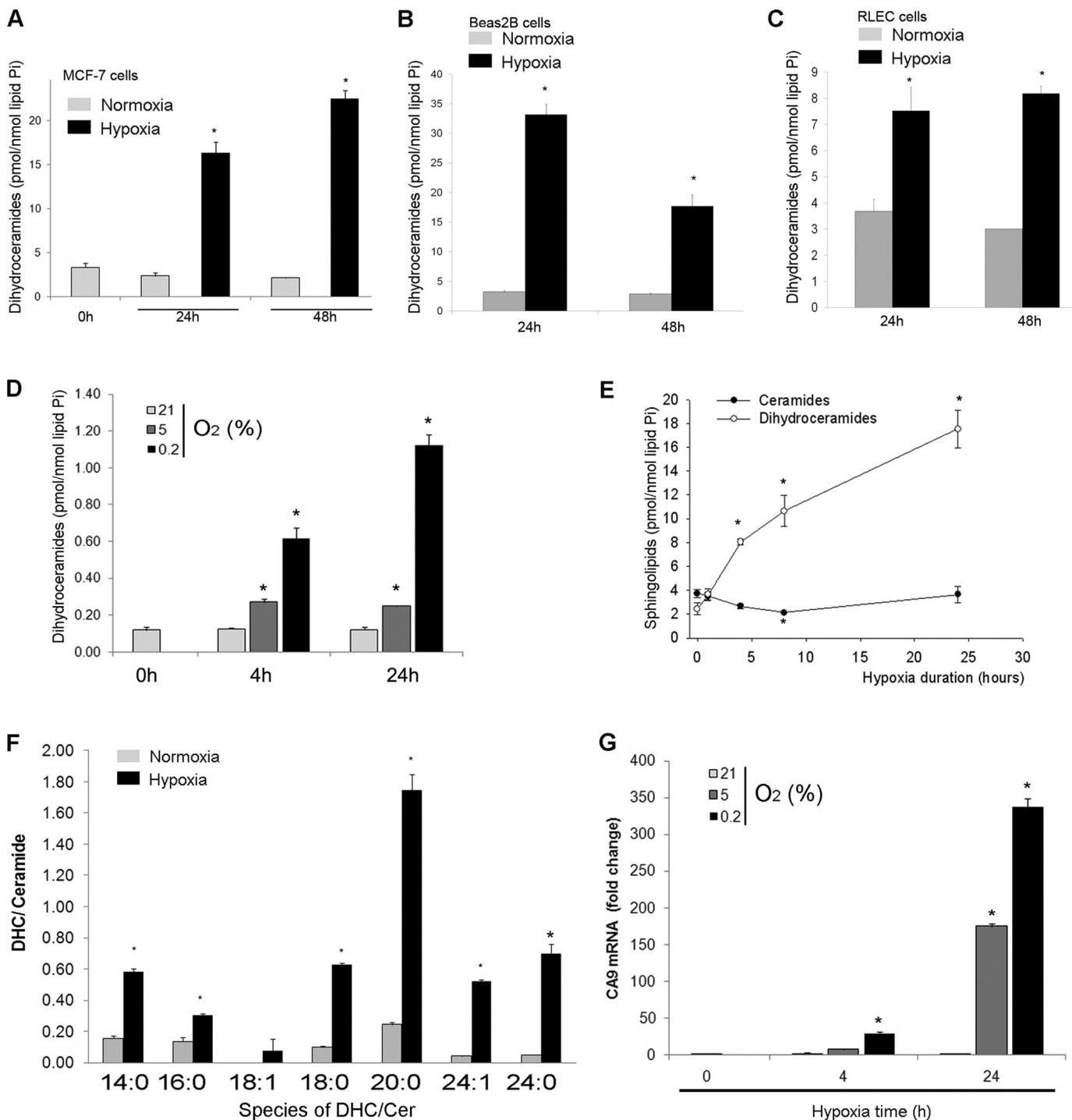


FIGURE 1. Profound up-regulation of DHC species upon exposure to hypoxia. A–C, DHC levels measured by mass spectrometry and normalized by lipid phosphorus (Pi) in either breast carcinoma (MCF-7; A), bronchial epithelial (Beas2B; B), or primary rat lung microvascular endothelial (RLEC) cells (C) after exposure to either normoxia (21% O₂; gray bars) or hypoxia (0.2% O₂; black bars) for 24 or 48 h (mean ± S.E.; **p* < 0.05 versus normoxia; *n* = 3). D, dose response of DHC levels in MCF-7 cells exposed to decreasing O₂ concentrations (21, 5, and 0.2%) for the indicated period of time (mean ± S.E.; **p* < 0.05 versus normoxia; *n* = 3). E, kinetics of ceramide (black circles) and DHC (white circles) levels in MCF-7 cells in response to hypoxia (0.2% O₂) (mean ± S.E.; **p* < 0.05 versus normoxia; *n* = 3). F, ratios of DHC/ceramide of individual species during normoxic (gray) or hypoxic (0.2% O₂ for 24 h; black bars) conditions in MCF-7 cells (mean ± S.E.; **p* < 0.05 versus normoxia; *n* = 3). G, carbonic anhydrase 9 (CA9) mRNA levels, a marker of hypoxia, measured by quantitative PCR in the samples described in D (mean ± S.E.; **p* < 0.05 versus normoxia; *n* = 3). Error bars, ± S.E.

additive increase in DHC, whereas inhibition of DEGS2 caused a synergistic increase in DHC levels (Fig. 3I). Studies of the abundance of mRNA encoding for key enzymes in the ceramide synthesis pathway demonstrated that their transcript levels either did not change (sphingomyelin synthase, ceramide syn-

thase-2 and -4, and ceramide kinase; data not shown) or actually increased during hypoxia (0.2% O₂ for 4–24 h) (serine palmitoyltransferase; data not shown).

Although many hypoxia-regulated responses are dependent on the activation of HIF, a variety of HIF-independent

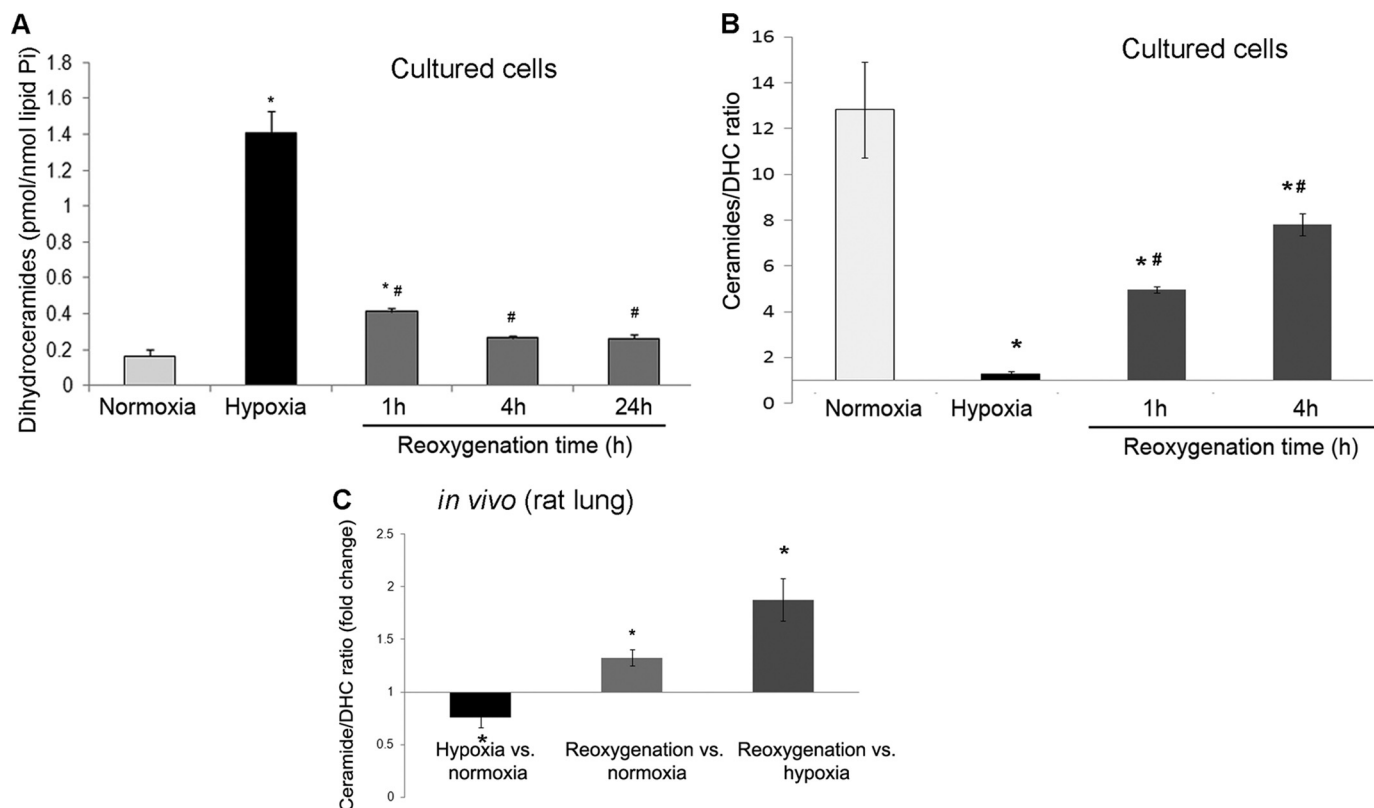


FIGURE 2. **Reoxygenation decreases DHC levels and increases ceramide levels *in vitro* and *in vivo*.** A and B, DHC levels (A) and ceramide/DHC ratios (B) in MCF-7 cells first subjected to 24 h of hypoxia (0.2% O₂; black bars) and then reintroduced to normal O₂ levels for the indicated times (mean \pm S.E.; *, $p < 0.05$ versus normoxia; #, $p < 0.05$ versus hypoxia; $n = 3$). C, ceramide/DHC ratio *in vivo* (-fold change versus indicated condition) in rat lung following exposure to hypoxia (5% O₂ for 60 min) or to reoxygenation (21% O₂ for 60 min) (mean \pm S.E.; *, $p < 0.05$ versus respective indicated conditions). Pi, phosphorus. Error bars, \pm S.E.

responses have also been described. We tested the role of HIF in the hypoxic up-regulation of the DHCs first in cells with genetic abnormalities of the HIF pathway. 786-O renal carcinoma cells carry an inactivated *VHL* gene and overexpress active HIF, which mimics HIF-dependent hypoxic conditions during normoxia (e.g. increased levels of the HIF-activated genes adrenomedullin and glucose transporter 1; Fig. 4A). Under normoxic conditions, both HIF-overexpressing (*VHL*-inactivated) cells and cells reconstituted with WT *VHL* (normal HIF levels) had similar DHC levels (Fig. 4B). This suggests that abnormal activation of HIF (as expected in hypoxia) is not sufficient to change the intracellular levels of DHC by itself. Next, we tested mouse embryonic fibroblast cells, which are HIF_{1 α} -null (demonstrated by the lack of carbonic anhydrase 9 up-regulation during hypoxia; Fig. 4C). Cells deficient in HIF were capable of inducing DHC after exposure to hypoxia (Fig. 4D), suggesting that HIF was not necessary for DHC up-regulation. Interestingly, HIF-deficient cells exhibited even higher DHC levels than HIF-sufficient cells, suggesting a potential negative regulatory effect of HIF on DHC up-regulation during hypoxia. Treatment of cells in normoxic conditions with the hypoxia mimetic and HIF prolyl hydroxylase inhibitor dimethylxalylglycine dramatically induced specific hypoxia-inducible genes carbonic anhydrase 9 (Fig. 4E) and VEGF-A (data not shown) but did not reproduce the hypoxic induction of DHCs (Fig. 4F), emphasizing the HIF independence of DHC up-regulation. These results indicate that although HIF may play a role in modulating DHC levels it is not the primary determinant of the DHC increase

under low oxygen tension. Because DHC desaturase activity is enhanced by NAD(P)H (23), we next tested the effect of pyruvate and 2-deoxyglucose, which are well established modifiers of NAD/NADH (24). Strikingly, these drugs did not significantly alter the response of sphingolipids to hypoxia (Fig. 4G), suggesting that physiologic changes in NAD/NADH levels do not have a direct impact on this particular activity of DEGS in live cells. Thus, the marked DHC increase observed in hypoxia may be directly mediated by the effect of oxygen on DHC desaturase.

Functional Effects of DHC and Ceramide Imbalances Induced by Hypoxia—Although initially regarded as biologically inactive precursors, recent reports indicate that DHCs are in fact bioactive lipids, although their effects may differ from those elicited by ceramides. Assessment of specific DHC functions is hampered by the fact that treatment with DHC induces the endogenous production of both DHC and ceramide (data not shown). However, treatment with the DHC analog C₁₂-dhCCPS has been demonstrated to specifically mimic the effect of DHC and to affect aspects of cell growth and proliferation (14, 15). The pleiotropic effects of hypoxia on the cell cycle and cell proliferation have been studied extensively (25). Whereas moderate levels of hypoxia can induce cell proliferation in multiple cell types, profound and/or prolonged hypoxia generally causes an inhibition of cell proliferation (26). We sought to investigate whether an increase in intracellular DHC in normoxic conditions could recapitulate the effects of profound hypoxia on cell proliferation. Treatment with the DHC analog C₁₂-dhCCPS in

Mechanism of Hypoxia-induced DHC

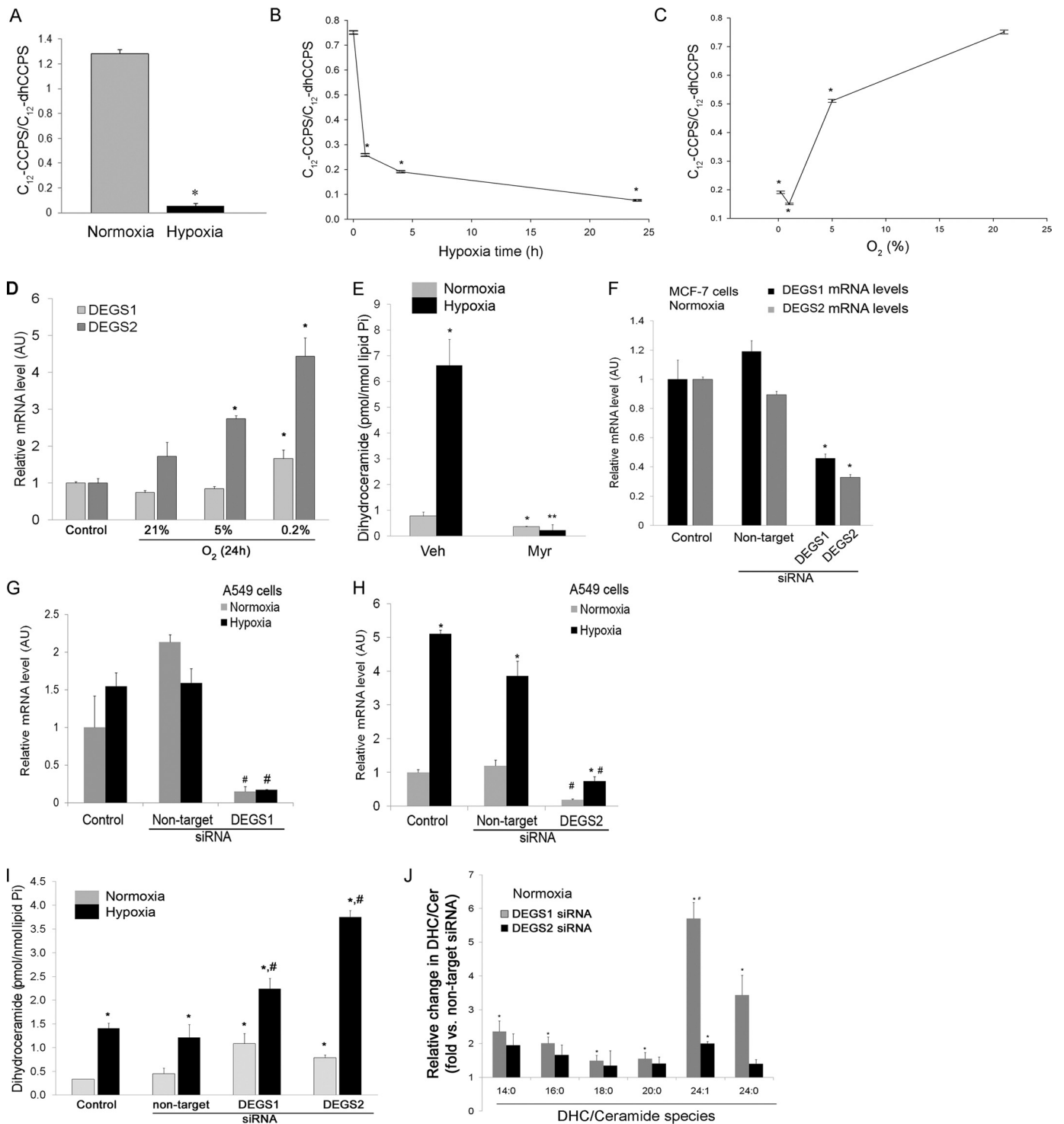


FIGURE 3. Inhibition of DHC desaturase activation induced by hypoxia increases DHC levels. A–C, endogenous DHC desaturase activity measured by the rate of conversion of a labeled DHC substrate to ceramide over the indicated times using mass spectrometry of lipids extracted from MCF-7 cells exposed to hypoxia as follows: 0.2% O_2 for 24 h (A); 0.2% O_2 over a time course (B); and O_2 dose response over 24 h (C) (mean \pm S.E.; *, $p < 0.05$ versus normoxia; $n = 3$). D, relative DEGS1 and DEGS2 mRNA levels determined by quantitative PCR in MCF-7 cells exposed to normoxia or hypoxia (5 or 0.2% O_2) for 24 h (mean \pm S.E.; *, $p < 0.05$ versus control (0 h of normoxia); $n = 3$). E, DHC levels in MCF-7 cells treated with control vehicle (Veh) or with myriocin (Myr), an inhibitor of serine palmitoyltransferase, followed by exposure to hypoxia (black bars; 0.2% O_2 for 24 h) (mean \pm S.E.; *, $p < 0.05$ versus normoxia; **, $p < 0.05$ versus hypoxia; $n = 3$). F–H, effective inhibition of DEGS1 or DEGS2 mRNA levels by specific siRNA during normoxia and hypoxia. F, DEGS1 (black bars) or DEGS2 (gray bars) mRNA levels in MCF-7 cells following transfection with DEGS1, DEGS2, or non-target siRNA (10 nM for 48 h) or left untreated (control) (*, $p < 0.05$ versus non-target siRNA; $n = 3$). DEGS1 (G) or DEGS2 (H) mRNA levels following normoxia (gray bars) or hypoxia (black bars; 1% O_2 for 24 h) exposure of A549 cells transfected with siRNA against DEGS1, DEGS2, or non-target siRNA (10 nM each for 48 h) or left untreated (control) (*, $p < 0.05$ versus normoxia; #, $p < 0.05$ versus non-target siRNA; $n = 3$). I, DHC levels in MCF-7 cells exposed to normoxia or hypoxia (1% O_2 for 24 h) after transfection with DEGS1, DEGS2, or non-target siRNA (10 nM) (mean \pm S.E.; *, $p < 0.05$ versus non-target siRNA; $n = 2$). J, fold change in DHC/ceramide ratios of individual species induced by DEGS1 (gray) or DEGS2 (black) knockdown compared with control MCF-7 cells (transfected with non-target siRNA) (mean \pm S.E.; *, $p < 0.05$ versus non-target siRNA; #, $p < 0.05$ versus DEGS2 siRNA; $n = 2$ –4). AU, arbitrary units. Error bars, \pm S.E.

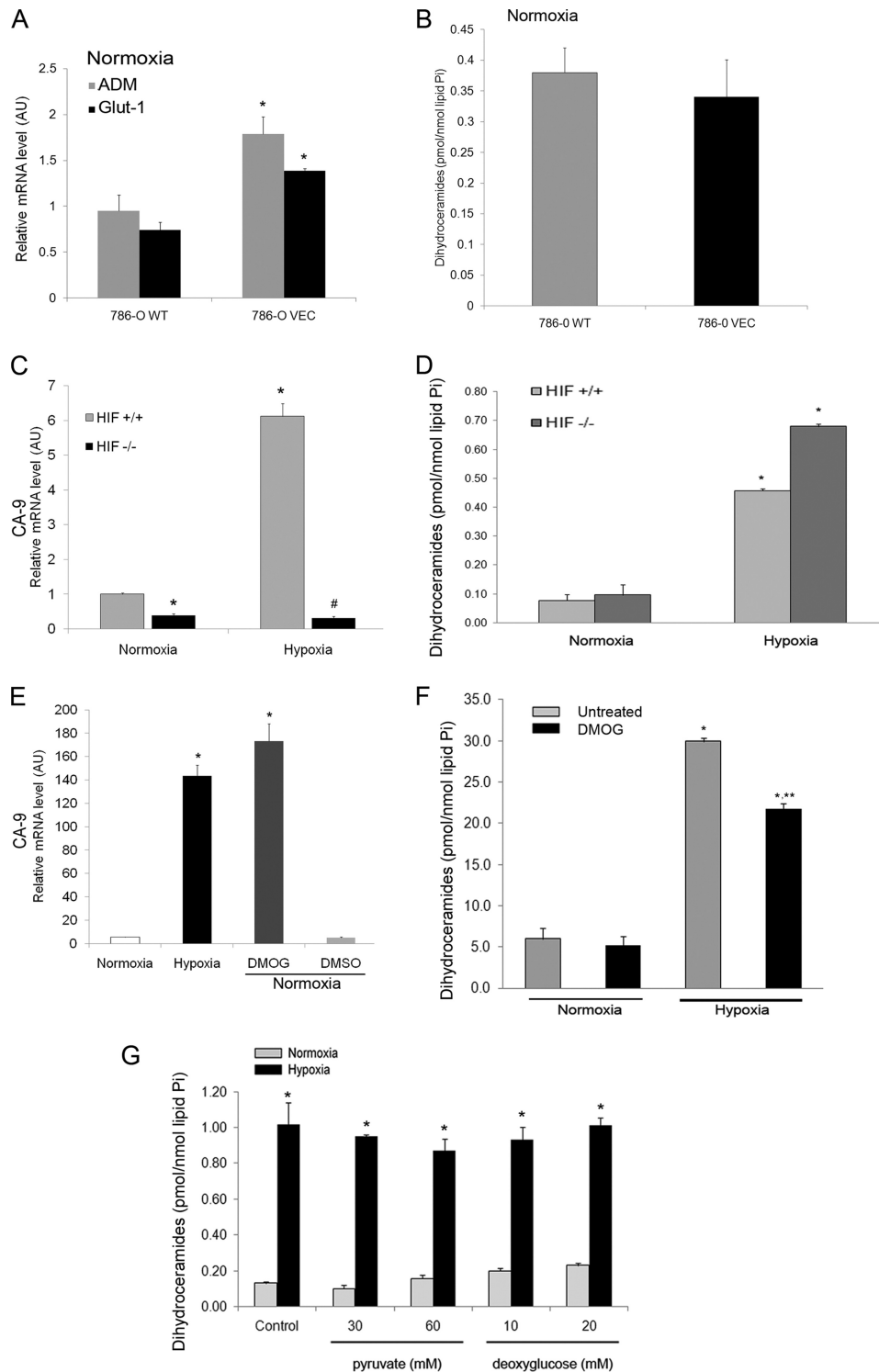


FIGURE 4. HIF- and NADH-independent up-regulation of DHC in hypoxia. *A*, adrenomedullin (*ADM*) (gray bars) and glucose transporter 1 (*Glut-1*) (black bars) mRNA levels, both markers of hypoxia, were measured by quantitative PCR in 786-O Vec renal carcinoma cells, which carry an inactivated *VHL* gene and overexpress active HIF, or in 786-O WT cells, which have normal HIF expression at 24 h of normoxia (*, $p < 0.05$ versus 786-O WT; $n = 3$). *B*, DHC levels following normoxia for 24 h in 786-O Vec (black bars) compared with 786-O WT (light gray bars) cells (mean \pm S.E.; no statistical difference was found when Student's *t* test was applied; $n = 3$). *C*, carbonic anhydrase 9 (*CA-9*) mRNA levels in HIF_{1 α} -deficient (black bars) or HIF_{1 α} -replete (gray bars) murine embryonic fibroblasts after exposure to normoxia or hypoxia (0.2% O₂ for 24 h) (mean \pm S.E.; *, $p < 0.05$ versus normoxic HIF^{+/+}; #, $p < 0.05$ versus hypoxic HIF^{+/+}; $n = 3$). *D*, DHC levels following normoxia or hypoxia (1% O₂ for 24 h) in HIF_{1 α} -deficient (dark gray bars) or HIF_{1 α} -replete (light gray bars) murine embryonic fibroblasts (mean \pm S.E.; *, $p < 0.05$ versus normoxia; $n = 3$). *E*, carbonic anhydrase 9 (*CA-9*) mRNA levels in MCF-7 cells after 24-h exposure to hypoxia (0.2% O₂; black bars), the HIF prolyl hydroxylase inhibitor dimethylxalylglycine (*DMOG*) (500 μ M; gray bars), or DMSO (0.5%; light gray bars) or left untreated (white bars) (*, $p < 0.05$ versus normoxia and versus DMSO; $n = 3$). *F*, DHC levels following treatment with the HIF prolyl hydroxylase inhibitor dimethylxalylglycine (*DMOG*) (500 μ M for 24 h; black bars) in MCF-7 cells exposed to either normoxia or hypoxia (0.2% O₂) (mean \pm S.E.; *, $p < 0.05$ versus normoxia; **, $p < 0.05$ versus hypoxia; $n = 2$). *G*, DHC levels following treatment with pyruvate (30 or 60 mM for 24 h) or 2-deoxyglucose (10 or 20 mM for 24 h) in MCF-7 cells exposed to either normoxia (gray bars) or hypoxia (1% O₂; black bars) (mean \pm S.E.; *, $p < 0.05$ versus normoxia; $n = 3$). *Pi*, phosphorus; *AU*, arbitrary units. Error bars, \pm S.E.

Mechanism of Hypoxia-induced DHC

both MCF-7 and A549 cells significantly and in a dose-dependent manner inhibited cell proliferation as measured by BrdU assays (Fig. 5, A and B, respectively), whereas treatment with ceramide C12:0 did not change cell proliferation (Fig. 5, A and B). These effects were noted to a greater extent during hypoxia (Fig. 5B). Similarly, knockdown of DEGS1 or DEGS2 by specific siRNAs (confirmed by quantitative PCR analysis of mRNA levels shown in Fig. 3) inhibited cell proliferation in both normoxic and hypoxic conditions compared with non-target siRNA-treated MCF-7 and A549 cells (Fig. 5, C and D). These results suggest that DHCs may be mediators of hypoxia-induced inhibitory effects on cell proliferation. To test whether we could reverse the above deleterious effect of hypoxia on cell proliferation, we established MCF-7 cell lines that express either DEGS1, DEGS2, or matching control vectors. The expression of FLAG-tagged protein in these cell lines was confirmed by Western blotting (Fig. 5E). As expected, cells overexpressing DEGS1 or DEGS2 exhibited an increased relative abundance of ceramides *versus* DHC in normoxic conditions (Fig. 5F). Importantly, a similar response was noted in cells exposed to hypoxia that overexpressed either DEGS1 or DEGS2; these cells exhibited an increased relative abundance of ceramides *versus* DHC as compared with matched control vector cell lines (Fig. 5G). Overexpression of either DEGS1 or DEGS2 significantly increased cell proliferation during hypoxia (Fig. 5H). These results indicate that overexpression of either DEGS protein was sufficient to overcome the negative impact of hypoxia on the cell proliferation response.

DISCUSSION

Our study characterizes for the first time *in vivo* the detailed responses of the DHC to ceramide conversion in the *de novo* ceramide synthesis pathway to a wide range of oxygen concentrations. We determined that the desaturation of DHCs acts as an HIF-independent biosensor to hypoxia in multiple primary and transformed cell types. Although the requirement for oxygen by the desaturases was established decades ago (21, 22, 26), the role of these enzymes in the response to physiologic hypoxia (rather than anoxia) in live cells has not been characterized in detail. Based on the amplitude and kinetics of DHC accumulation at physiologic alterations of oxygen concentrations, the enzymatic desaturation step within the *de novo* ceramide pathway fulfills the criteria of an oxygen sensor.

Structural crystallography (27) as well as Mossbauer and extended x-ray absorption fine structure spectroscopy provided important clues with respect to the presence of oxygen at the core of DEGS enzymes with two oxygen atoms forming an "oxo bridge" with two iron ions, which are directly involved in the desaturation reaction (28). However, direct utilization of oxygen does not necessarily predict the dynamic range of activity in response to changes in oxygen concentrations. Several relevant analogies can be made with the two major classes of oxygen-dependent prolyl hydroxylases. First, analogously to DEGS, both HIF and collagen prolyl hydroxylases bind oxygen directly (29, 30). The corresponding K_m values of the HIF-modifying forms are slightly above the atmospheric concentration of oxygen (31), affording a uniquely dynamic response across a physiological range of oxygen tensions that fits their role as

oxygen sensors (32, 33). In sharp contrast, the collagen prolyl hydroxylases exhibit a much lower K_m , allowing optimal hydroxyprolyl collagen synthesis even under severe hypoxia, and are therefore not regarded as sensors (34). Second, similarly to the HIF prolyl hydroxylases, desaturases can also perform hydroxylation in addition to desaturation (35); however, of the two DEGS isoforms, only DEGS2 exhibits significant C-4 hydroxylase activity (36). Finally, similarly to HIF prolyl hydroxylases, both DEGS transcripts increased in abundance with prolonged hypoxia exposure, which may reflect a compensatory feedback mechanism.

Most studies of DEGS function have concentrated on DEGS1, whereas DEGS2 has received much less attention. As previously mentioned, DEGS2 is generally regarded as a hydroxylase rather than a desaturase; however, it conceivably acts on the same pool of DHCs as DEGS1. Our data indicate that in our models oxygen catalyzes the conversion of comparable amounts of DHC via either isoform. In addition to their up-regulation by hypoxia, DHCs have also been shown to be increased by oxidative stress (37). We can speculate that reactive oxygen species might affect the redox status of iron at the core of DEGS1 similarly to their demonstrated effect on the corresponding iron at the core of HIF prolyl hydroxylases (38).

There is limited knowledge with regard to alterations in ceramide metabolism pathways under hypoxic conditions. A recent study using *C. elegans* showed that loss of ceramide synthase markedly increased the sensitivity of this organism to anoxia (4). Interpreted in the context of our data, the decrease in DHCs rather than or in addition to the ceramide synthase-mediated decrease in ceramides might be involved in a decreased ability to survive anoxic injury. In addition, our study identifies DEGS as a novel molecular target by which hypoxia regulates mammalian cellular responses. In previous studies, hypoxia was found to increase ceramides in neurons, and the mechanism proposed was serine palmitoyltransferase induction (9). We confirmed a requirement of serine palmitoyltransferase induction to activate the *de novo* pathway of ceramide synthesis and DHC production. Similar to our findings, a recent report identified an accumulation of DHC in human colon cancer cells exposed to long term hypoxia (1% O₂ for 7 days) (39). These reports highlight the universal response of DHC accumulation to hypoxia across species and tissues for which we now provide a direct mechanism.

The biological effects of DHCs are distinct from those of ceramides (12). In our experiments, indirect augmentation of DHCs either by siRNA blockade of DEGS1 or DEGS2 or direct treatment with DHC decreased cell proliferation. Therefore, DHC up-regulation during normoxia recapitulated the effect of profound and/or prolonged hypoxia in most primary and several transformed cell lines (25). Additionally, DHCs may actively preserve cell viability with one potential mechanism being increased autophagy (39), which is emerging as a protective response under low oxygen tension. However, the fast reconversion of DHC into ceramides (complete after 1 h of reoxygenation) may indicate that the hypoxia-induced accumulated pool of DHCs may contribute to the harmful release of intracellular ceramides, which are implicated as mediators of several models of ischemia-reperfusion injury (40). Given the

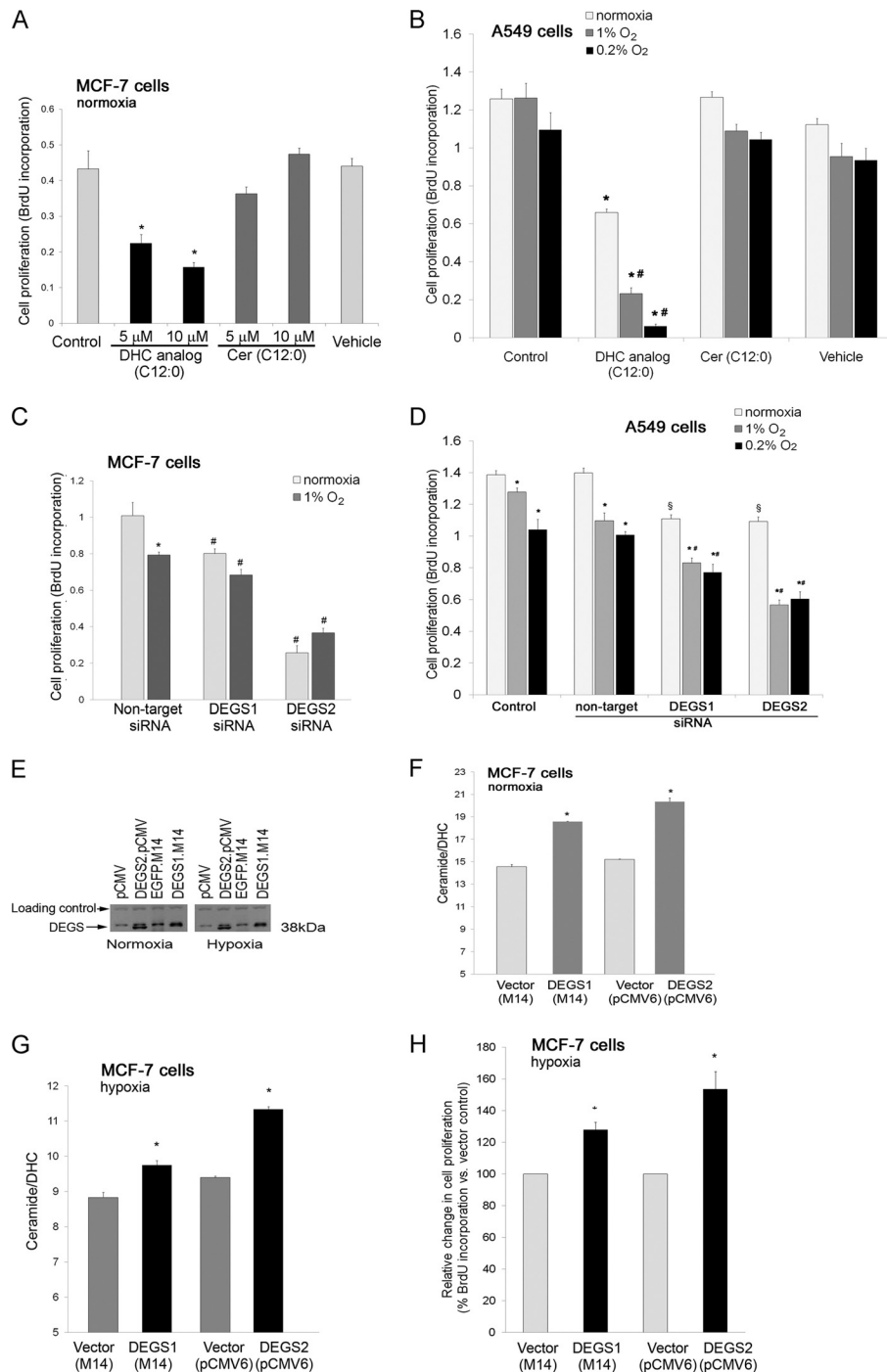


FIGURE 5. DHC accumulation decreases cell proliferation. *A*, cell proliferation measured by BrdU incorporation in MCF-7 cells exposed to normoxia and treated with DHC analog C₁₂-dhCCPS (5 or 10 μ M for 24 h; *black bars*), ceramide C12:0 (5 or 10 μ M for 24 h; *dark gray bars*), or vehicle for ceramide (0.1% ethanol; *light gray bars*) (mean \pm S.E.; *, $p < 0.05$ versus control; $n = 5$ for each assay). *B*, cell proliferation measured by BrdU incorporation in A549 cells exposed to normoxia (*light gray bars*) or hypoxia (1% O₂ (*dark gray bars*) or 0.2% O₂ (*black bars*)) and treated for 48 h with DHC analog C₁₂-dhCCPS (10 μ M), ceramide C12:0 (10 μ M), or vehicle for ceramide (0.1% ethanol) (mean \pm S.E.; *, $p < 0.05$ versus vehicle or control; #, $p < 0.05$ versus hypoxia-control; $n = 5$ for each assay). *C*, cell proliferation measured by BrdU incorporation in MCF-7 cells exposed for 48 h to normoxia (*light gray bars*) or hypoxia (1% O₂; *dark gray bars*) after treatment with non-target, DEGS1, or DEGS2 siRNA (mean \pm S.E.; *, $p < 0.05$ versus normoxia; #, $p < 0.05$ versus non-target siRNA; $n = 5$). *D*, cell proliferation measured by BrdU incorporation in A549 cells exposed for 24 h to normoxia (*light gray bars*) or hypoxia (1% O₂ (*dark gray bars*) or 0.2% O₂ (*black bars*)) after treatment with non-target, DEGS1, or DEGS2 siRNA or left untreated (control) (mean \pm S.E.; *, $p < 0.05$ versus non-target in each respective group; #, $p < 0.05$ versus hypoxia-control; §, $p < 0.05$ versus normoxia-control; $n = 5$ for each assay). *E*, MCF-7 cells were stably transfected with the following plasmids: pCMV6, DEGS2.pCMV, EGFP.M14, or DEGS1.M14; subjected to normoxia or hypoxia (1% O₂) for 24 h; and then analyzed by Western blotting using an anti-FLAG antibody. The molecular mass of DEGS1 and DEGS2 is 38 kDa. The upper band represents nonspecific anti-FLAG binding as a loading control. *F*, ceramide/DHC ratio in MCF-7 cells transfected with pCMV6, DEGS2.pCMV, EGFP.M14, or DEGS1.M14 (10 μ g each) followed by exposure to normoxia for 24 h (mean \pm S.E.; *, $p < 0.05$ versus respective control vector). *G*, ceramide/DHC ratio in MCF-7 cells transfected with pCMV6, DEGS2.pCMV, EGFP.M14, or DEGS1.M14 (10 μ g each) followed by exposure to hypoxia (1% O₂ for 24 h) (mean \pm S.E.; *, $p < 0.05$ versus respective control vector; $n = 2$). *H*, cell proliferation measured by BrdU incorporation in MCF-7 cell lines stably transfected with pCMV, DEGS2.pCMV, EGFP.M14, or DEGS1.M14 and then exposed to hypoxia (1% O₂ for 24 h). Results are expressed as relative increase (percent) versus respective control vector (mean \pm S.E.; *, $p < 0.05$ versus control vector; $n = 5$). Error bars, \pm S.E.

Mechanism of Hypoxia-induced DHC

relative magnitude of ceramide increases during reoxygenation relative to that of DHC decreases, it is very likely that other pathways, such as sphingomyelin hydrolysis, may also significantly contribute to the ceramides released during reperfusion.

In conclusion, we describe for the first time a general mechanism of ceramide response to hypoxia based on the blockade of DHC conversion into desaturated ceramide forms. The elevation of DHCs caused by desaturase inhibition may be a useful, easily quantifiable biomarker of hypoxia. Furthermore, the resulting shift in balance between the DHC and ceramide may govern cell proliferation and death responses in hypoxia and reoxygenation.

Acknowledgment—We acknowledge Marjorie Albrecht for expert technical assistance.

REFERENCES

1. Kaelin, W. G., Jr., and Ratcliffe, P. J. (2008) *Mol. Cell* **30**, 393–402
2. Ye, J., and Koumenis, C. (2009) *Curr. Mol. Med.* **9**, 411–416
3. Bartke, N., and Hannun, Y. A. (2009) *J. Lipid Res.* **50**, (suppl.) S91–S96
4. Menuz, V., Howell, K. S., Gentina, S., Epstein, S., Riezman, I., Fornallaz-Mulhauser, M., Hengartner, M. O., Gomez, M., Riezman, H., and Martinou, J. C. (2009) *Science* **324**, 381–384
5. Noureddine, L., Azzam, R., Nemer, G., Bielawski, J., Nasser, M., Bitar, F., and Dbaibo, G. S. (2008) *Prostaglandins Other Lipid Mediat.* **86**, 49–55
6. Bhuiyan, M. I., Islam, M. N., Jung, S. Y., Yoo, H. H., Lee, Y. S., and Jin, C. (2010) *Biol. Pharm. Bull.* **33**, 11–17
7. Liu, J., Ginis, I., Spatz, M., and Hallenbeck, J. M. (2000) *Am. J. Physiol. Cell Physiol.* **278**, C144–C153
8. Merrill, A. H., Jr. (2002) *J. Biol. Chem.* **277**, 25843–25846
9. Kang, M. S., Ahn, K. H., Kim, S. K., Jeon, H. J., Ji, J. E., Choi, J. M., Jung, K. M., Jung, S. Y., and Kim, D. K. (2010) *Cell. Signal.* **22**, 610–618
10. Cogolludo, A., Moreno, L., Frazziano, G., Moral-Sanz, J., Menendez, C., Castañeda, J., González, C., Villamor, E., and Perez-Vizcaino, F. (2009) *Cardiovasc. Res.* **82**, 296–302
11. Kendler, A., and Dawson, G. (1992) *J. Neurosci. Res.* **31**, 205–211
12. Crowder, C. M. (2009) *Science* **324**, 343–344
13. Stiban, J., Fistere, D., and Colombini, M. (2006) *Apoptosis* **11**, 773–780
14. Kravka, J. M., Li, L., Szulc, Z. M., Bielawski, J., Ogretmen, B., Hannun, Y. A., Obeid, L. M., and Bielawska, A. (2007) *J. Biol. Chem.* **282**, 16718–16728
15. Szulc, Z. M., Bielawski, J., Gracz, H., Gustilo, M., Mayroo, N., Hannun, Y. A., Obeid, L. M., and Bielawska, A. (2006) *Bioorg. Med. Chem.* **14**, 7083–7104
16. Ryan, H. E., Poloni, M., McNulty, W., Elson, D., Gassmann, M., Arbeit, J. M., and Johnson, R. S. (2000) *Cancer Res.* **60**, 4010–4015
17. Kibel, A., Iliopoulos, O., DeCaprio, J. A., and Kaelin, W. G., Jr. (1995) *Science* **269**, 1444–1446
18. Bligh, E. G., and Dyer, W. J. (1959) *Can. J. Biochem. Physiol.* **37**, 911–917
19. Dobrowsky, R. T., and Kolesnick, R. N. (2001) *Methods Cell Biol.* **66**, 135–165
20. Petrache, I., Natarajan, V., Zhen, L., Medler, T. R., Richter, A. T., Cho, C., Hubbard, W. C., Berdyshev, E. V., and Tuder, R. M. (2005) *Nat. Med.* **11**, 491–498
21. Livak, K. J., and Schmittgen, T. D. (2001) *Methods* **25**, 402–408
22. Michel, C., van Echten-Deckert, G., Rother, J., Sandhoff, K., Wang, E., and Merrill, A. H., Jr. (1997) *J. Biol. Chem.* **272**, 22432–22437
23. Geeraert, L., Mannaerts, G. P., and van Veldhoven, P. P. (1997) *Biochem. J.* **327**, 125–132
24. Garofalo, O., Cox, D. W., and Bachelard, H. S. (1988) *J. Neurochem.* **51**, 172–176
25. Huang, L. E. (2008) *Cell Death Differ.* **15**, 672–677
26. Carmeliet, P., Dor, Y., Herbert, J. M., Fukumura, D., Brusselmans, K., Dewerchin, M., Neeman, M., Bono, F., Abramovitch, R., Maxwell, P., Koch, C. J., Ratcliffe, P., Moons, L., Jain, R. K., Collen, D., and Keshert, E. (1998) *Nature* **394**, 485–490
27. McDonough, M. A., Li, V., Flashman, E., Chowdhury, R., Mohr, C., Liénard, B. M., Zondlo, J., Oldham, N. J., Clifton, I. J., Lewis, J., McNeill, L. A., Kurzeja, R. J., Hewitson, K. S., Yang, E., Jordan, S., Syed, R. S., and Schofield, C. J. (2006) *Proc. Natl. Acad. Sci. U.S.A.* **103**, 9814–9819
28. Buist, P. H. (2004) *Nat. Prod. Rep.* **21**, 249–262
29. Ivan, M., Kondo, K., Yang, H., Kim, W., Valiano, J., Ohh, M., Salic, A., Asara, J. M., Lane, W. S., and Kaelin, W. G., Jr. (2001) *Science* **292**, 464–468
30. Jaakkola, P., Mole, D. R., Tian, Y. M., Wilson, M. I., Gielbert, J., Gaskell, S. J., von Kriegsheim, A., Hebestreit, H. F., Mukherji, M., Schofield, C. J., Maxwell, P. H., Pugh, C. W., and Ratcliffe, P. J. (2001) *Science* **292**, 468–472
31. Hirsilä, M., Koivunen, P., Günzler, V., Kivirikko, K. I., and Myllyharju, J. (2003) *J. Biol. Chem.* **278**, 30772–30780
32. Epstein, A. C., Gleadle, J. M., McNeill, L. A., Hewitson, K. S., O'Rourke, J., Mole, D. R., Mukherji, M., Metzzen, E., Wilson, M. I., Dhanda, A., Tian, Y. M., Masson, N., Hamilton, D. L., Jaakkola, P., Barstead, R., Hodgkin, J., Maxwell, P. H., Pugh, C. W., Schofield, C. J., and Ratcliffe, P. J. (2001) *Cell* **107**, 43–54
33. Ward, J. P. (2008) *Biochim. Biophys. Acta* **1777**, 1–14
34. Myllyharju, J. (2008) *Ann. Med.* **40**, 402–417
35. Broadwater, J. A., Whittle, E., and Shanklin, J. (2002) *J. Biol. Chem.* **277**, 15613–15620
36. Munoz-Olaya, J. M., Matabosch, X., Bedia, C., Egido-Gabás, M., Casas, J., Llebaria, A., Delgado, A., and Fabriàs, G. (2008) *Chem. Med. Chem.* **3**, 946–953
37. Idkowiak-Baldys, J., Apraiz, A., Li, L., Rahmaniyan, M., Clarke, C. J., Kravka, J. M., Asumendi, A., and Hannun, Y. A. (2010) *Biochem. J.* **427**, 265–274
38. Pan, Y., Mansfield, K. D., Bertozzi, C. C., Rudenko, V., Chan, D. A., Giaccia, A. J., and Simon, M. C. (2007) *Mol. Cell Biol.* **27**, 912–925
39. Signorelli, P., Munoz-Olaya, J. M., Gagliostro, V., Casas, J., Ghidoni, R., and Fabriàs, G. (2009) *Cancer Lett.* **282**, 238–243
40. Cuzzocrea, S., Di Paola, R., Genovese, T., Mazzon, E., Esposito, E., Crisafulli, C., Bramanti, P., and Salvemini, D. (2008) *J. Pharmacol. Exp. Ther.* **327**, 45–57